



Stewart, J. P., Klimis, N., Savvaidis, A., Theodoulidis, N., Zargli, E., Athanasopoulos, G., ... Margaris, B. (2014). Compilation of a local  $V_s$  profile database and its application for inference of  $V_{s30}$  from geologic- and terrain-based proxies. *Bulletin of the Seismological Society of America*, 104(6), 2827-2841. <https://doi.org/10.1785/0120130331>

Publisher's PDF, also known as Version of record

Link to published version (if available):

[10.1785/0120130331](https://doi.org/10.1785/0120130331)

[Link to publication record in Explore Bristol Research](#)

PDF-document

This is the final published version of the article (version of record). It first appeared online via Seismological Society of America at <http://doi.org/10.1785/0120130331>. Please refer to any applicable terms of use of the publisher.

## University of Bristol - Explore Bristol Research

### General rights

This document is made available in accordance with publisher policies. Please cite only the published version using the reference above. Full terms of use are available: <http://www.bristol.ac.uk/pure/about/ebr-terms>

# *Bulletin of the Seismological Society of America*

This copy is for distribution only by  
the authors of the article and their institutions  
in accordance with the Open Access Policy of the  
Seismological Society of America.

For more information see the publications section  
of the SSA website at [www.seismosoc.org](http://www.seismosoc.org)



THE SEISMOLOGICAL SOCIETY OF AMERICA  
400 Evelyn Ave., Suite 201  
Albany, CA 94706-1375  
(510) 525-5474; FAX (510) 525-7204  
[www.seismosoc.org](http://www.seismosoc.org)

# Compilation of a Local $V_S$ Profile Database and Its Application for Inference of $V_{S30}$ from Geologic- and Terrain-Based Proxies

by Jonathan P. Stewart, Nikolaos Klimis, Alexandros Savvaidis, Nikos Theodoulidis, Elena Zargli, George Athanasopoulos, Panagiotis Pelekis, George Mylonakis,\* and Basil Margaris

**Abstract** The time-averaged shear-wave velocity in the upper 30 m of a site ( $V_{S30}$ ) is commonly used for ground-motion prediction. When measured velocities are unavailable,  $V_{S30}$  is estimated from proxy-based relationships developed for application on global or local scales. We describe the development of a local relationship for Greece, which begins with compilation of a profile database (PDB) from published sources and engineering reports. The PDB contains 314 sites; 238 have profile depths  $\geq 30$  m and 59 are within 100 m of accelerographs. We find existing relations for extrapolating a time-averaged velocity for depths less than 30 m to  $V_{S30}$  to over-predict  $V_{S30}$ . We present equations for these extrapolations.

We then compile proxies for PDB sites, including terrain type, surface geology, and surface gradients at 30 and 3 arcsec resolution (from radar-derived digital elevation models [DEMs]). When checked against ground survey data, we find ground elevations from 3 arcsec DEMs to be more accurate relative to survey data than alternative 30, 9, and 1 arcsec DEMs. Drawing upon expert opinion, we develop geologic categories based on age, gradation, and depositional environment and assign such categories to PDB sites. We find an existing 30 arcsec gradient-based global model to be biased relative to local  $V_{S30}$  data for gradients  $> \sim 0.05$  m/m. Bias relative to a California model is also found for four of the eight well-populated geomorphic categories, and new (local) values are provided. We find statistically significant effects of the 3 arcsec gradient on  $V_{S30}$  for Quaternary and Tertiary materials but no gradient effect for those from the Mesozoic. Among Quaternary sediments, Holocene, mapped Quaternary (age unspecified), and mixed/fine-gradation materials exhibit consistent  $V_{S30}$ -gradient trends, whereas Pleistocene and coarse-gradation sediments have faster velocities. For the study region, we recommend use of the modified terrain- and geology-based methods in combination for proxy-based  $V_{S30}$  estimation.

*Online Material:* Profile database (spreadsheet) and figures of elevation residuals.

## Introduction

Most ground-motion prediction equations (GMPEs) for major tectonic regimes worldwide use  $V_{S30}$  as the principal parameter representing site condition for the engineering characterization of site amplification. Arguments for and against  $V_{S30}$  have been presented elsewhere (Borcherdt, 1994; Castellaro *et al.*, 2008; Seyhan *et al.*, 2014), which we will not repeat here. A premise for our work is simply that  $V_{S30}$  is a required parameter for the development and implementation

of most major GMPEs, including those of the Next Generation Attenuation (NGA) projects (Bozorgnia *et al.*, 2014).

The most straightforward way to evaluate  $V_{S30}$  for a given site is to measure seismic velocities to a depth of at least 30 m (deeper profiles are typically desirable to develop more complete insights of site response, but  $V_{S30}$  strictly requires a profile that is only 30 m deep). In this case,  $V_{S30}$  is simply computed as the ratio of 30 m to the shear-wave travel time through the upper 30 m of the site profile. When no geophysical data are available for a given site,  $V_{S30}$  is estimated from proxies, which may be based on geomorphology (using ground slope or terrain categories; Wald and Allen, 2007, and Yong *et al.*, 2012, respectively), geology (e.g.,

\*Also at University of California, Los Angeles, Department of Civil and Environmental Engineering; and also at University of Patras, Department of Civil Engineering, Patras, Greece.

Wills and Clahan, 2006), or geotechnical site categories (Chiou *et al.*, 2008; Seyhan *et al.*, 2014). The Wald and Allen (2007) proxy relationship is intended for global application in the sense that its proxy of ground slope at 30 arcsec resolution is globally available, and the correlation of slope to  $V_{S30}$  uses a global dataset.

Our objective in this paper is to develop local data resources and predictive tools that can be used within the study region (in this case, Greece) to estimate  $V_{S30}$ . The presumption is that such local relationships are more accurate and reliable within the applicable region than global methods. We begin by presenting a substantial profile database (PDB) developed from sources in the open literature, research reports, professional engineering reports, and personal communications. Each site in the PDB has geophysical measurements and is categorized according to proxies. We anticipate this database will be a useful product in its own right for engineering applications and future proxy-related research. We then utilize the PDB to test existing methods in the literature for extrapolating  $V_{SZ}$  (time-average velocity to depth  $z_p$ ) to  $V_{S30}$  when profile depths ( $z_p$ ) are less than 30 m. This extrapolation can be performed with relatively high confidence and substantially expands the size of the database.


The principal technical question that we address is the manner by which  $V_{S30}$  can be estimated from available proxies. We consider the proxies of surface geology, surface gradient, and geomorphic site categories. We describe a process by which geologic categories representative of local conditions were assigned to sites using the best-available, relatively large-scale geologic maps for Greece. We then test existing proxies for  $V_{S30}$  estimation using the PDB and, after finding shortcomings, develop recommended proxy-based relationships for  $V_{S30}$  prediction in the study region.

Using the results of this work, we develop protocols for assigning  $V_{S30}$  values and their related uncertainties to specific locations (e.g., strong-motion stations) in Greece that are of interest. These protocols are also expected to be directly useful for hazard or risk-mapping efforts within the study region when reliable geophysical data are unavailable. Moreover, the methodology developed here should be useful for other regions worldwide where there is a significant reliance on proxies for estimating site parameters.

## Profile Database

### Site Selection and Database Contents


The PDB is an inventory of sites in Greece where geophysical measurements have been undertaken to develop shear-wave velocity ( $V_S$ ) profiles. To be included in the PDB, the profile depth must be at least 5–6 m and the data must be considered generally reliable, given local knowledge and generally accepted norms for geophysical testing. The PDB includes a relatively broad range of test types: crosshole, downhole (including seismic cone penetration tests), active and passive surface-wave methods, and seismic refraction.

As with the Pacific Earthquake Engineering Research Center Next Generation Attenuation of Ground Motions site database (Seyhan *et al.*, 2014), we exclude refraction-microtremor-type measurements due to probable bias in  $V_S$  at depth. Inferred  $V_S$  profiles from penetration resistance data are not considered. Aside from the availability of a usable  $V_S$  profile of sufficient depth, the only other criteria for including a site in the PDB were that the measurement location be known (location is shown on the site plan or coordinates are provided) and that the data are available for use (either because it is already published or we obtained permission for its use).  The PDB is given in Table S1 (available in the electronic supplement to this article). Figure 1 shows the locations of sites in the PDB overlaid on a geology map of Greece.

A number of sites in the PDB have relevant information beyond the  $V_S$  profile, such as a geotechnical borehole log and/or a description of local geology based on field observations by a geologist. Figure 2 shows a typical example of the available information for a site in the PDB (site number THETHE005b), including geophysical logs, borehole logs, and penetration resistance data.

The sites included in the PDB include the following:

- Strong-motion stations, many of which have been geophysically characterized for ground-motion studies. Where applicable, the distance of the profile to the nearest accelerometer is indicated in the PDB. Of the 314 sites in the PDB, 59 are located very near (within 100 m) accelerometers, and an additional 83 accelerometer sites are located within 1.0 km of a site in the PDB and have similar geology (according to Institute of Geological and Mineral Exploration [IGME] geologic maps at a scale of 1:50,000).
- Sites characterized as part of local microzonation projects or seismic-hazard/risk studies. In such cases, although  $V_{S30}$  is often mapped throughout a local area, we consider only the source measurements, not inferences of  $V_{S30}$  between measurements.
- Locations of civil infrastructure projects such as major buildings, industrial facilities, refineries, dams, pipelines, highways, tunnels, bridges, and harbors. In such cases, we utilize geotechnical design reports containing  $V_S$  profile data.
- Sites characterized as part of forensic investigations of heavily damaged regions following earthquakes (e.g., Thessaloniki, Argostoli, Aegio, Athens, Kalamata, the Kozani and Grevena area, Lefkada, and others).

 The data source for each site in the PDB is indicated in Table S1 and includes journal and conference papers, research reports, private engineering consulting offices, and government offices.

The principal contents of the PDB are an identifier code, location (geodetic coordinates), metadata on the geophysical testing (data source, measurement type, profile depth), time-averaged shear-wave velocities over various depths (details below), surface geologic information (mapped description,



**Figure 1.** Geologic map of Greece showing locations of sites in profile database (PDB) and locations of strong-motion stations in site database. The geologic map used here is from digital sources (for ease of plotting) with a scale of 1:500,000. This map is for illustrative purposes only; higher-resolution maps were used to assign geologic conditions to particular sites. The color version of this figure is available only in the electronic edition.

assigned code, map source), ground slope gradients for 30 and 3 arcsec map resolutions, and geomorphic-terrain categories per Iwahashi and Pike (2007). Details on the shear-wave velocity data, slope gradients, and terrain categories are given in the following subsections. Geologic categories are described in the next section.

#### $V_S$ Profile Data

Velocities shown in the PDB are  $V_{SZ}$  and  $V_{S30}$ . Velocity  $V_{SZ}$  is the time-averaged shear-wave velocity to profile depth  $z_p$  and can be computed as

$$V_{SZ} = \frac{z_p}{\Delta t_z}, \quad (1)$$

in which

$$\Delta t_z = \int_0^{z_p} \frac{dz}{V_S(z)}. \quad (2)$$

$\Delta t_z$  is the travel time for shear waves from depth  $z_p$  to the ground surface, and the integral is evaluated in practice through summation across velocities taken as constant within depth intervals. When the  $V_S$  profile extends to depths of 30 m or greater,  $V_{S30}$  can be computed directly from the profile data by replacing  $z_p$  with 30 m in equations (1) and (2).

When  $z_p < 30$  m,  $V_{S30}$  cannot be calculated directly; this applies to 76 of the 314 sites in the PDB. Estimation of  $V_{S30}$  for these 76 sites requires  $V_{SZ}$ -to- $V_{S30}$  extrapolation conditioned on profile depth  $z_p$ . Procedures for extrapolations of this type have been proposed by Boore (2004) and Boore *et al.* (2011) based on the analysis of  $V_S$  profile data principally from California and Japan, respectively. Here, we

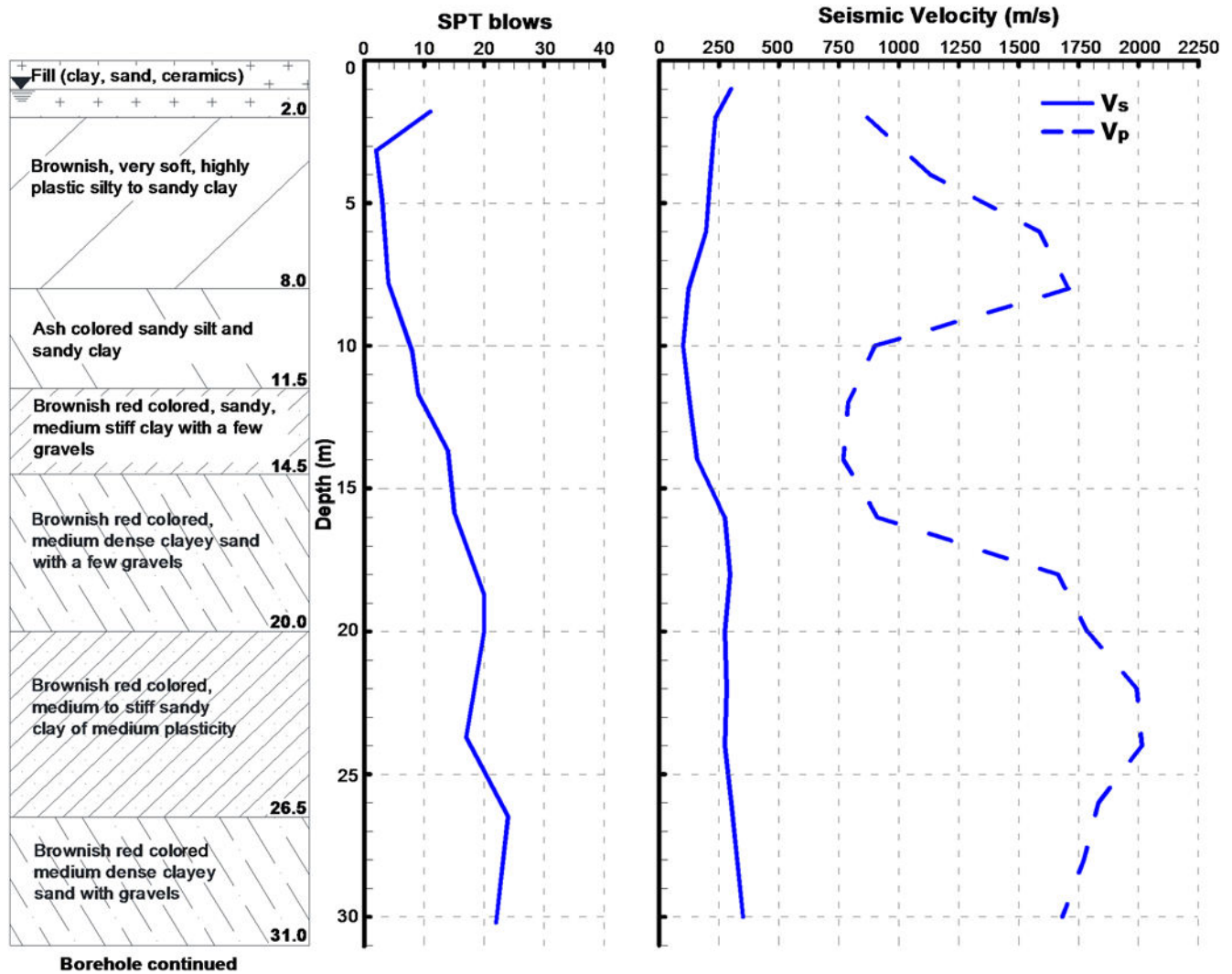


**Figure 2.** Example of compiled information for one site (THETHE005b) in the PDB, including seismic velocity profiles, geotechnical log, and penetration resistance. The velocity profiles in this case were derived from downhole logging. The color version of this figure is available only in the electronic edition.

test the applicability of these methods to the Hellenic data. We use 202 of the 238 sites in the PDB with  $z_p \geq 30$  m (the additional 36 sites are excluded because the geophysics only provided  $V_{S30}$  and not shallower velocities), along with 23 additional sites that were excluded from the PDB solely because of unknown location (i.e., the profiles are good quality and have  $z_p \geq 30$  m).

Figure 3 shows plots of  $V_{SZ}$  against  $V_{S30}$  for the 225 Hellenic sites for values of  $z_p = 5, 10, 14,$  and  $20$  m. The results generally indicate slower  $V_{S30}$  values for a given  $V_{SZ}$  from the Hellenic data as compared to the prior models, suggesting somewhat flatter velocity gradients on average from the Hellenic data. This discrepancy is greatest for the 5 m data, for which only the Boore *et al.* (2011) model has coefficients we can use for comparison. The large misfit in this case is expected because the prior model is considered applicable for relatively firm rock conditions in Japan (specifically K-NET sites with  $z_p \approx 10$  m), in which the velocity

gradients near the surface are often relatively steep. Because of the persistent differences, including at larger profile depths, we elected to not adopt the prior results, but instead fit the data with a linear relationship as shown in Figure 3 and given by

$$\log(V_{S30}) = c_0 + c_1 \log(V_{SZ}). \quad (3)$$

A parabolic function was also considered but was not adopted because it produced results very similar to the linear function. In almost all cases, the prior models fall outside the confidence intervals of the present fits, suggesting statistically significant differences between the Hellenic data and the prior relations. Table 1 provides coefficients  $c_0$  and  $c_1$  for various profile depths between 5 and 28 m. Error term  $\sigma_e$  is the standard deviation of the fit residuals.

Because many of the sites in the PDB have profile depths  $z_p > 30$  m, it is also possible to use the data to investigate

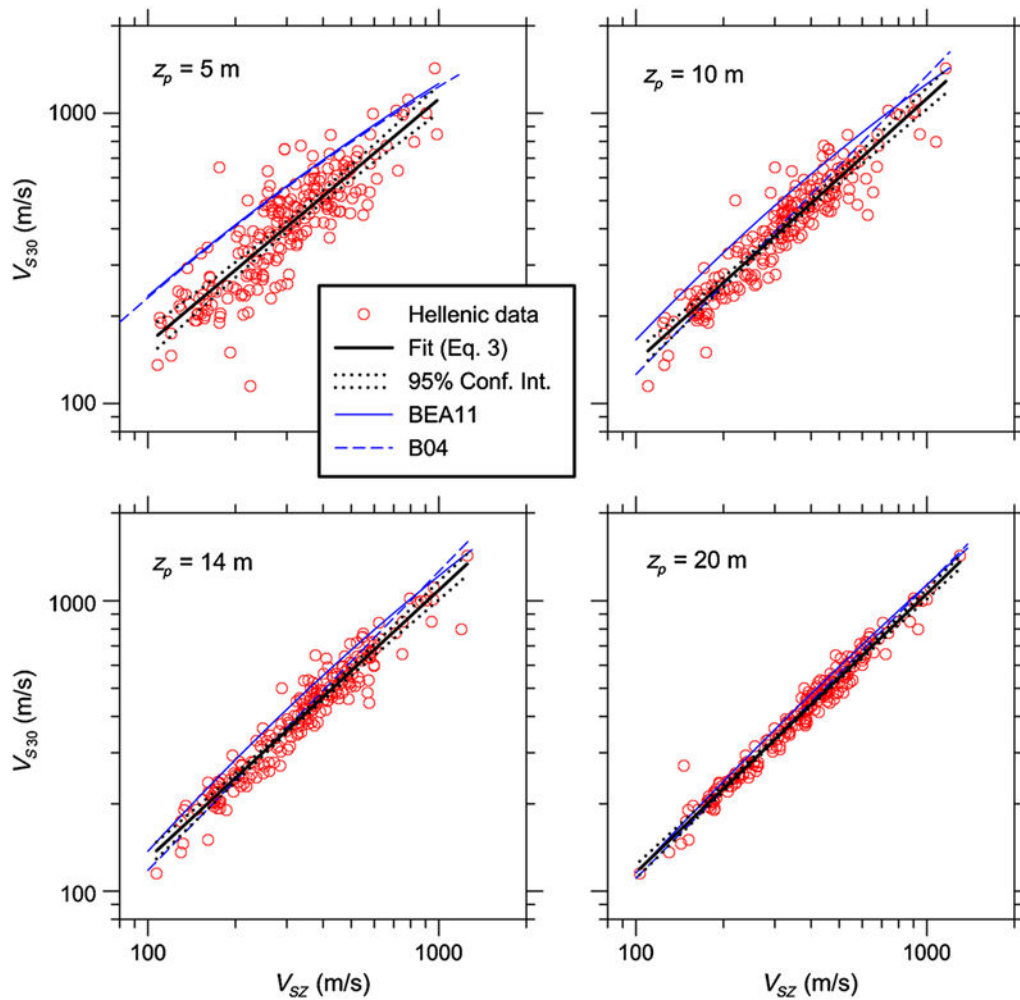


**Figure 3.** Comparison of  $V_{SZ}$ – $V_{S30}$  data from Greece with relationships developed by Boore (2004; shown as B04) and Boore *et al.* (2011; shown as BEA11). Linear fits through Hellenic data are shown with 95% confidence intervals. The color version of this figure is available only in the electronic edition.

the degree to which  $V_{S30}$  is correlated with deeper velocity structure. Figure 4 illustrates the relationship between  $V_{S30}$  and  $V_{S60}$ , which is possible for 24 sites. As shown in the figure, the two velocities are strongly correlated, with a coefficient of determination ( $R^2$ ) of 0.94. This is very similar to

results obtained previously for Japan by Boore *et al.* (2011), who investigated depths as great as 600 m. This correlation of  $V_{S30}$  with deeper velocity structure explains why  $V_{S30}$ , which is fundamentally a metric of the shallow site condition, has been found to correlate well with site response at low frequencies involving wavelengths much longer than 30 m.

**Table 1**  
Model Coefficients for  $V_{SZ}$ -to- $V_{S30}$  Extrapolation

$z_p$ (m)	$c_0$	$c_1$	$\sigma_e$
5	0.522	0.842	0.233
10	0.331	0.907	0.156
12	0.287	0.919	0.138
14	0.261	0.925	0.121
16	0.240	0.930	0.107
18	0.165	0.955	0.086
20	0.144	0.960	0.076
22	0.088	0.978	0.054
24	0.064	0.984	0.045
26	0.038	0.991	0.033
28	0.014	0.997	0.015

### Ground Slope Gradients

The aforementioned slope gradients are based on digital elevation models (DEMs), which are available worldwide at various resolutions (30, 9, 3, and 1 arcsec) from the Shuttle Radar Topography Mission (SRTM; specific web resources used to access DEMs for the four resolution levels are indicated in the [Data and Resources](#)). For example, an SRTM map at 3 arcsec resolution will have a value for elevation on a grid of points separated horizontally by 3 arcsec in latitude and longitude. Gradients are computed by differencing elevations for adjacent points and dividing by horizontal

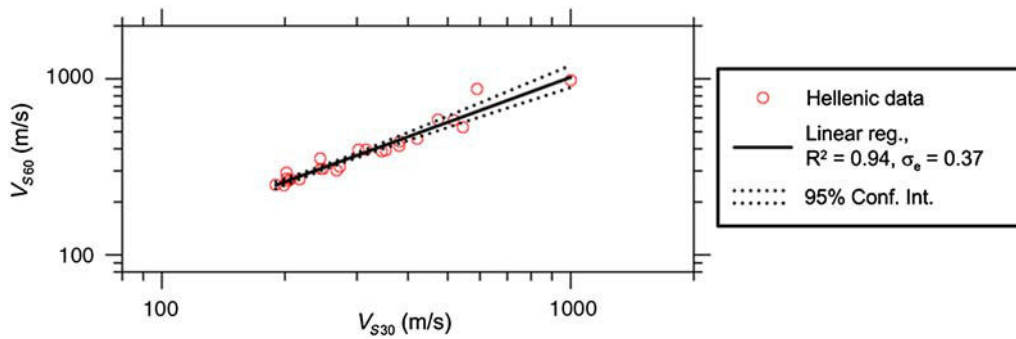


**Figure 4.** Relationship between  $V_{S60}$  and  $V_{S30}$  using Hellenic data. The color version of this figure is available only in the electronic edition.

separation distance. Given the gridded pattern of elevations, gradients can be measured in eight horizontal directions to adjacent points. To be consistent with past practice, we use the maximum of these eight gradients as computed from the *gradgradient* command in Generic Mapping Tool software (see [Data and Resources](#)). This process produces a map of gradients at the same level of resolution as the underlying DEM; the gradient for a given site is taken from the nearest grid point.

An important consideration when compiling gradients for proxy-based  $V_{S30}$  estimation is the level of horizontal resolution used in the gradient calculation. There are two critical factors affecting this choice: (1) possible bias in the gradient calculation and (2) the predictive power of the gradient for  $V_{S30}$ . We address the reliability of gradient calculations for the study region here; the effectiveness of gradients of different resolutions for  $V_{S30}$  estimation is examined subsequently.

Although the reliability of gradient calculations would appear to be enhanced at higher resolutions, canopy effects (e.g., from vegetation or buildings) can bias point estimates of elevations from high-resolution maps and, by extension, gradients measured from elevation changes. For example, [Allen and Wald \(2009\)](#) found gradients from 9 arcsec SRTM DEMs to be poorly resolved at low gradients, which was attributed to canopy effects. They considered gradients from 30 arcsec DEMs to be less affected by such effects “because the small-scale variations in elevation that are abundant in the high-resolution data are smoothed” (p. 940).

To evaluate the reliability of DEM-based elevations at different resolutions for our study region, we compiled elevations measured from ground-surveyed stations in the National Trigonometric Network (Hellenic Military Geographical Service; see [Data and Resources](#)) for comparison to the DEM elevations. [Figures S1 and S2](#) show a representative example of elevation residuals ( $\Delta z$  is the surveyed elevation minus DEM elevations) versus surveyed elevation for resolutions of 1, 3, 9, and 30 arcsec for rural and urban areas in and surrounding Larissa (central Greece). The results show positive bias in elevations at all levels of resolution, but the smallest bias, and lowest standard deviation of residuals, occurs at 3 arcsec resolution. For the nonurban region ([Fig. S1](#)), bias and dispersion of  $\Delta z$  are highest at 30 arcsec

resolution (24 and 50 m, respectively) and decrease with increasing resolution to minimums of 7.5 m (mean) and 6.8 m (standard deviation) at 3 arcsec resolution. The bias and dispersion then increase for the finest resolution considered of 1 arcsec (19 and 11 m, respectively), which we interpret as a canopy effect similar to that observed previously by [Allen and Wald \(2009\)](#) for other regions. The principal difference from that prior work is the level of map resolution at which the canopy effect becomes most evident (9 arcsec in the prior work, 1 arcsec here). The data for the urban region ([Fig. S2](#)) are relatively sparse due to its smaller size, but the same trends are evident.

On the basis of these findings, we consider gradients for elevations of 3 and 30 arcsec in the proxy development work to follow. We do not consider the 1 arcsec data due to the evidence of bias from canopy effects.

#### Terrain Categories

Application of the geomorphology-based scheme of [Iwahashi and Pike \(2007\)](#) requires information on gradient, convexity, and texture. Gradient is obtained from 30 arcsec SRTM maps, as described in the previous subsection. Local convexity, an expression of surface curvature, was derived by (1) applying a  $3 \times 3$  Laplacian filter on DEM elevation to identify convex (positive curvature), concave (negative curvature), and planar (zero curvature) regions and (2) computing the percentage of convex cells within a 10-cell radius from any DEM grid node. Surface texture was computed by (1) identifying pits and peaks from the difference map between the original DEM and its smoothed version derived from  $3 \times 3$  median filtering and (2) counting the number of pits and peaks within a 10-cell radius from any DEM grid node. The above three layers of geometric characteristics were then used in an automated classification framework to define 16 terrain classes using an iterative nested-means algorithm. The resulting 16 classes ([Fig. 5a](#)) range from steep (classes 1, 2, 3, 4) to gentle (classes 13, 15, 14, 16) according to the local DEM slope gradient, and from fine texture high convexity (classes 1, 5, 9, 13) to coarse texture low convexity (classes 4, 8, 12, 16), according to the other two terrain variables. Because the classification is automated, no region-specific



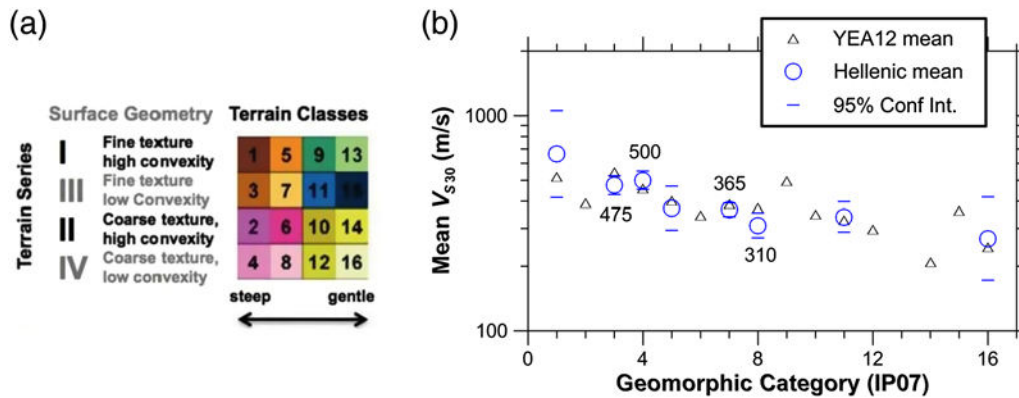


**Figure 5.** (a) Depiction of Iwahashi and Pike (2007) terrain categories; (b) category mean  $V_{S30}$  values as given by Yong *et al.* (2012; shown as YEA12) and from the Hellenic PDB (with confidence intervals). Numbers for categories 3, 4, 7, and 8 are category means judged sufficiently different from the YEA12 values that a change to these values is provided for applications in Greece. The color version of this figure is available only in the electronic edition.

geomorphological label can be assigned to terrain classes, although such labels could be developed based on local knowledge.

### Geologic Categories

This section concerns the use of surface geology as a proxy for  $V_{S30}$  estimation within Greece. Mountrakis (1985) and Higgins and Higgins (1996) provide an overview of Hellenic geology. The use of geology-related proxies to estimate  $V_{S30}$  has been surprisingly limited in scope worldwide. In California, Wills and Clahan (2006) developed 19 geologic categories for the state (many specific to certain regions) and computed  $V_{S30}$  statistics (mean and standard deviations) for profiles within those categories. That work was extended by Wills and Gutierrez (2008) to replace Quaternary categories with bins defined by 3 arcsec gradients, while retaining the use of categories for rock sites (Tertiary and Mesozoic). Scasserra *et al.* (2009) checked  $V_{S30}$  values for an Italian database against the category means of Wills and Clahan (2006), finding general compatibility for Quaternary categories but differences for older units. Similar to Wills and Clahan (2006), Matsuoka *et al.* (2006) defined categories they describe as geomorphic, but which we interpret to be more geologic in their description (e.g., mountain tertiary and alluvial fan), and compute  $V_{S30}$  statistics for applicable profiles within each category. Lee *et al.* (2001) related  $V_{S30}$ -based site categories to surface geologic conditions in Taiwan. Kottke *et al.* (2012) present preliminary relations between mean  $V_{S30}$  and 19 geologic categories in the central and eastern United States, although the data were only sufficient to provide stable means for nine of the categories. Within Greece, Zargli *et al.* (2013) investigate the relationship between geology, terrain, and slope gradient at 30 arcsec resolution but do not investigate relationships to  $V_{S30}$ . Outside of the aforementioned areas, we are not aware of other efforts in the archival literature to relate  $V_{S30}$  to geology.

Critical considerations associated with the use of geology as a  $V_{S30}$  proxy are map resolution and the consistency of mapping across the study region. Both of these issues presented challenges in the development of a geology-related proxy. The principal factor affecting resolution for paper-based maps is scale, which varies from 1:500,000 to 1:5000 in Greece. The largest scale available for the entire territory is 1:50,000 in 325 maps by the IGME (see Data and Resources). The consistency of these maps is relatively poor in the sense that the geologic terms used to describe units (lithostratigraphic and structural names) are not standardized, which results from the geologic mapping upon which the maps are based having occurred over a period of six decades by various geologists. A particular problem is that the currently used model for the geotectonic zones of Greece was developed after 1970 (Nikolakopoulos and Tsombos, 2010). There are many examples of adjacent geologic maps depicting different conditions at their boundaries, especially if one map predates the 1970 geotectonic model and its neighbor is more recent.

Despite these challenges with consistency, we utilize the IGME maps due to their relatively good resolution and general availability. Following extensive internal discussions and consultation with an experienced panel of geologists (listed in Acknowledgments), we developed the set of categories descriptive of depositional environment and material gradation shown in Table 2. These conditions can be related to the much more diverse set of geologic terms used on the maps to describe units (the total number of mapped units on the source maps is 69). The conversion of the 69 mapped units to those given in Table 2 was by expert opinion of the authors and our team of geologists. Accordingly, the PDB shows the geology as-mapped for each site, including age and lithostratigraphic description, and our interpretation of the geology based on the depositional environment and gradation as given in Table 2.

The site categorization with respect to gradation is motivated by a general understanding that fine-grained

Table 2  
Categories of Grain Gradation and Deposition Environment

Grain Gradation	Deposition Environment
1. Coarse grained	A. Nonmarine
2. Fine grained	Terrestrial: (1) desert, (2) loess
3. Mixed grained	Subaqueous: (3) fluvial, (4) lacustrine, (5) paludal, (6) spelean
	Glacial: (7) subglacial, (8) glacier-terminus, (9) estuarine
	B. Transitional
	(10) Deltaic
	(11) Lagoonal
	(12) Estuarine
	C. Marine
	Coastal: (13) beach, (14) tidal-flat, (15) muddy shoreline, (16) reefy shoreline, (17) prodelta
	Shelf: (18) siliciclastic, (19) carbonate
	Abyssal: (20) continental slope, (21) submarine canyon/fan/abyssal plain, (22) open deep ocean

sediments tend to have lower seismic velocities than coarse-grained sediments, with mixed gradation being an intermediate case. The use of gradation-based categories, especially for Quaternary sediments, is well established in prior work (e.g., Fumal, 1978; Fumal and Tinsley, 1985; Stewart *et al.*, 2003). The categorization by depositional environment is motivated by practicality (this information is often directly indicated on geologic maps) and a general understanding that high-energy depositional environments (e.g., fast-flowing streams) produce coarser and stiffer sediments than do low-energy environments (e.g., lakes, bays, or seas). The categorization of geologic conditions according to depositional environment for ground-motion or seismic velocity studies has strong precedent in the literature (e.g., Borchardt, 1970; Park and Elrick, 1998; Stewart *et al.*, 2003; Wills and Clahan, 2006).

Figure 1 shows the 314 sites in the PDB relative to a map indicating geologic age. The map used in the figure is relatively small scale (1:500,000) for illustrative purposes, but the actual age assigned to a site in the PDB is based on the 1:50,000 IGME maps. The major age groups and the number of PDB sites in each are given in Table 3. A significant majority of the sites are Quaternary (Holocene, Pleistocene, or mapped Quaternary). The depositional environment classes of fluvial (class 3) and lacustrine (class 4) dominate the PDB sites, with 210 and 55 occurrences, respectively. Material gradations are more uniformly distributed, with 85 coarse, 46 fine, and 172 mixed occurrences.

Table 3  
Breakdown of Sites in PDB According to Geologic Age

Geologic Age	Number of Sites
Holocene	94
Pleistocene	61
Mapped Quaternary (more specific age unknown)	67
Tertiary: Neogene	63
Mesozoic and Paleozoic	29

### Proxy-Based $V_{S30}$ Estimation

In this section, we test existing methods for  $V_{S30}$  estimation using terrain- and gradient-related proxies. Some revisions to the terrain mean  $V_{S30}$  values are provided as a result of misfits. We then develop a  $V_{S30}$  estimation procedure based on geology and gradient.

#### Terrain and Gradient

Wald and Allen (2007) use the proxy of ground slope gradient at 30 arcsec resolution to estimate  $V_{S30}$  using global data segregated into active crustal regions and stable continental regions (the data for active regions were from California, Italy, Taiwan, and Utah). The data indicate increasing  $V_{S30}$  with increasing gradient. The Yong *et al.* (2012) procedure for estimating  $V_{S30}$  considers gradient and geomorphologic factors related to convexity and texture. Those factors are jointly analyzed using an automated topography classification scheme by Iwahashi and Pike (2007) to segregate terrain

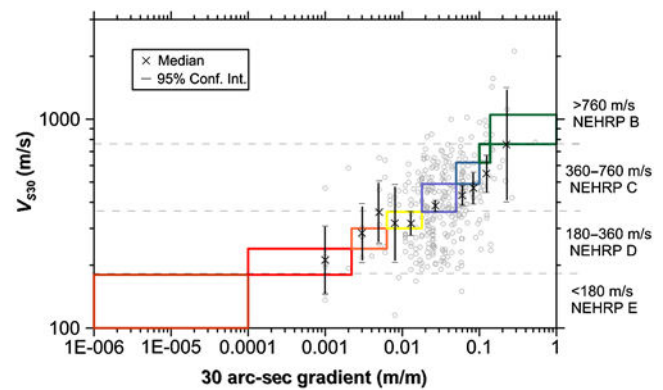
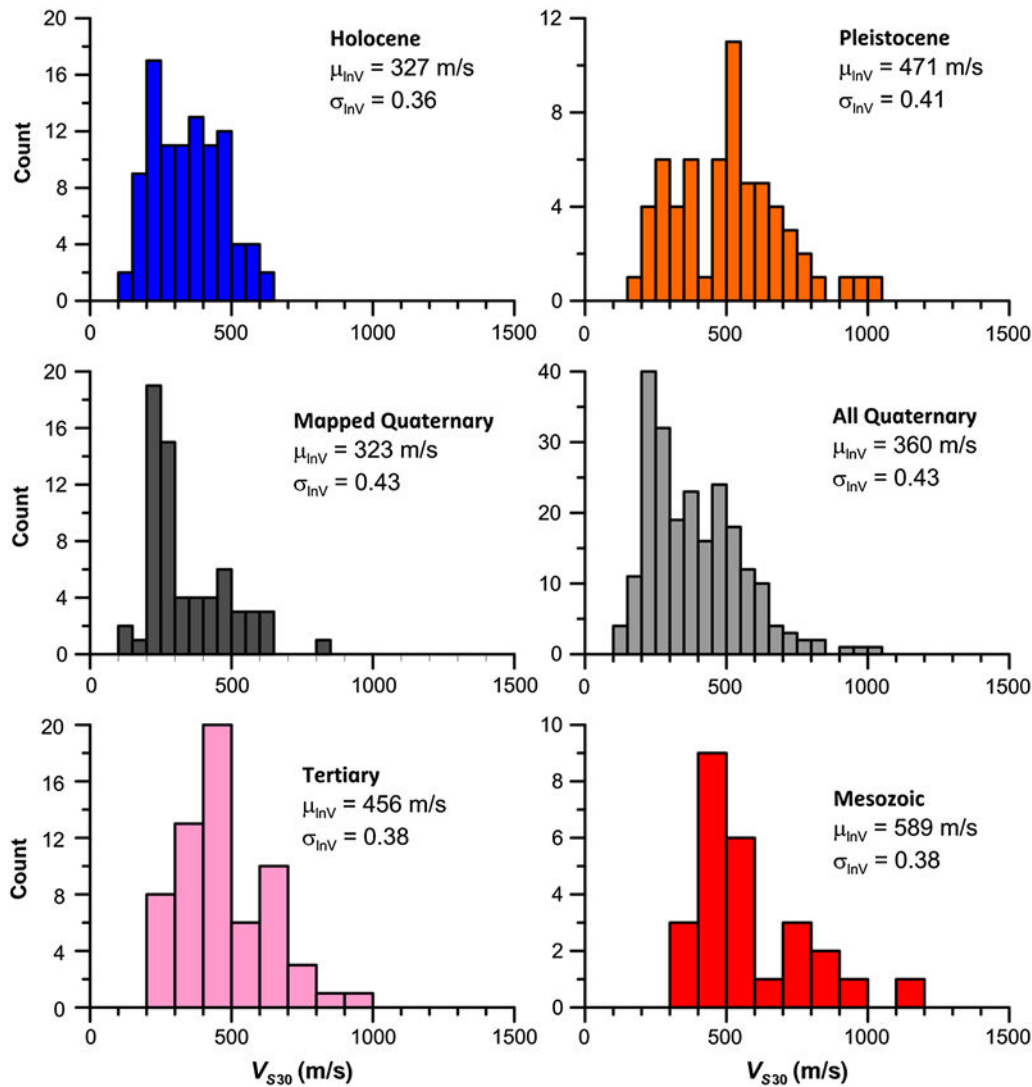


Figure 6. Trends of  $V_{S30}$  against a 30 arcsec gradient using data from Greece as compared to ranges for active crustal regions provided by Wald and Allen (2007). Binned means of data are shown with their 95% confidence interval. The color version of this figure is available only in the electronic edition.



**Figure 7.**  $V_{S30}$  values from the PDB, sorted by geologic age.  $\mu_{\ln V}$  is the exponent of the mean of the logs of  $V_{S30}$ , whereas  $\sigma_{\ln V}$  is the standard deviation of the logs. The color version of this figure is available only in the electronic edition.

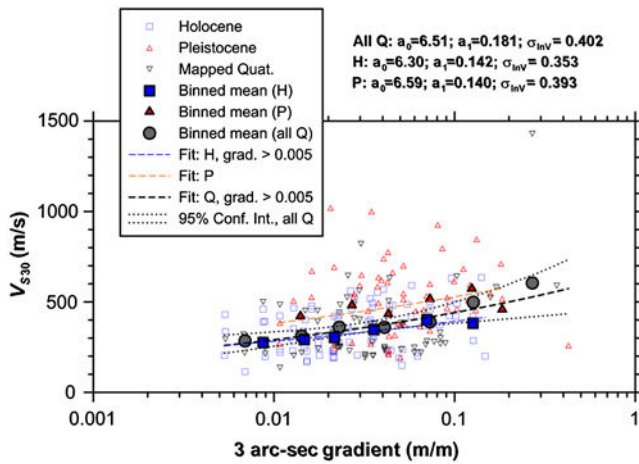
types into 16 categories, which were then linked by [Yong et al. \(2012\)](#) to log-average  $V_{S30}$  values within the categories using data from California.

Figure 6 shows the ranges of  $V_{S30}$  provided by [Wald and Allen \(2007\)](#) as a function of the 30 arcsec gradient, along with the data from the Hellenic PDB. Also shown are  $V_{S30}$  means and their 95% confidence intervals within approximately equally spaced gradient bins (on a log scale). We find the slope gradient proxy-based estimates to be unbiased with respect to the Hellenic data for relatively flat slopes (gradient  $< \sim 0.05$  m/m). For sites with steeper gradients, there is a slight overprediction bias. The bias of the model for steeper gradients is significantly less than that found for California data by [Seyhan et al. \(2014\)](#) but is reasonably consistent with what has been found for European data as a whole by [Lemoine et al. \(2012\)](#). This prior European study included few of our sites, so the present analysis comprises a largely independent check of the method. On the basis of these results, application

of the 30 arcsec gradient proxy can be supported. However, as discussed further below, for the study region we are recommending a combination of gradient and geology in lieu of gradient alone. With regard to geomorphic site categories, we have computed mean  $V_{S30}$  values (specifically, the exponent of the mean of the logs) of the Hellenic data within each category and show the results in Figure 5b, along with their 95% confidence intervals. Also shown in the figure are the values provided by [Yong et al. \(2012\)](#) based on California data. For categories for which the California means fall very near or outside the confidence intervals for the mean of the Hellenic data, we update the category means based on the Hellenic database with the new values marked in the figure.

#### Geology-Based Proxy

*Age- and Gradient-Based Analysis.* In this section, we describe the relationship between geology and  $V_{S30}$  using data



**Figure 8.**  $V_{S30}$  compared with gradient for Quaternary data, with binned means and fit curves per power law relationship (equation 4). 95% confidence intervals for Quaternary fit encompass the Holocene fit, suggesting the difference is not statistically significant, whereas the Pleistocene fit is at faster velocities that are generally above the confidence intervals. The color version of this figure is available only in the electronic edition.

from the PDB with the intention of developing recommendations specific to the study region for proxy-based estimation of  $V_{S30}$ . To begin, Figure 7 shows histograms of  $V_{S30}$  for different geologic age categories. For the Quaternary, we separately consider those sites mapped as Quaternary (i.e., no information on whether age is Holocene or Pleistocene), sites mapped into the Holocene or Pleistocene age groups, and all Quaternary (Holocene, Pleistocene, and mapped Quaternary). Through visual inspection, the histogram shape is considered to be better represented as log normal than normal, so we compute the mean and standard deviation of logs, which are written as  $\mu_{\ln V}$  and  $\sigma_{\ln V}$ , respectively.

When compared with California (Wills and Clahan, 2006), the mean  $V_{S30}$  values from Greece are generally higher than the California values for Quaternary (and its subsets) and Mesozoic formations (which are mostly Cretaceous for California). The California and Hellenic mean  $V_{S30}$  values are similar for Tertiary formations.

We parsed the data in various ways to investigate factors beyond age affecting  $V_{S30}$ , including gradient (at 30 and 3 arcsec resolution), depositional environment, and gradation (per Table 2). Figure 8 shows  $V_{S30}$  against 3 arcsec gradient for Quaternary sediments. For flat gradients ( $< \sim 0.015$ ), the data are dominated by the Holocene and mapped Quaternary units. For gradients of approximately 0.015–0.15, all categories are present, with Holocene data having slower velocities. In the same figure, we also show binned means ( $\mu_{\ln V}$ ; four bins per log cycle of gradient) for Holocene, Pleistocene, and all Quaternary data. The Holocene and Quaternary trends are very similar before diverging ( $Q$  being higher) beyond a gradient of about 0.1. Pleistocene velocities are consistently higher and have a similar dependence on gradient.

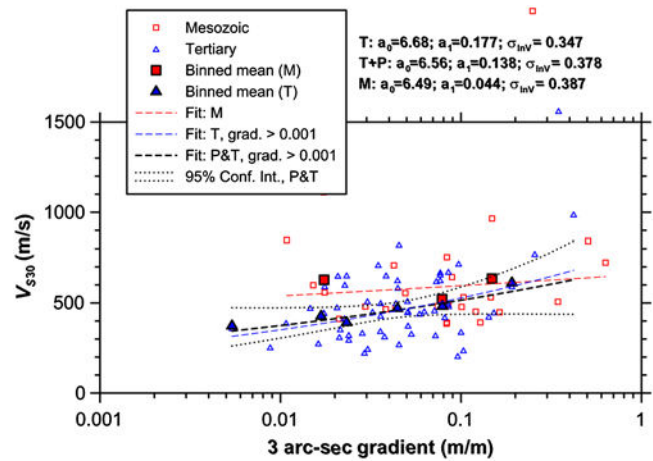


**Figure 9.**  $V_{S30}$  compared with gradient for Tertiary (T) and Mesozoic (M) data, with binned means and fit curves per power law relationship (equation 4). Because the Tertiary results are similar to those from the Pleistocene (P), these categories are combined with the resulting fit shown (P&T). Note that the Tertiary fit is well within the 95% confidence intervals for the combined P&T results. The Mesozoic fit is at faster velocities generally above the P&T confidence intervals and has no significant trend with gradient. The color version of this figure is available only in the electronic edition.

We fit the following power law relationship through three data sets (all Quaternary, Holocene, and Pleistocene):

$$\overline{\ln(V_{S30})} = a_0 + a_1 \ln(s), \quad (4)$$

in which  $V_{S30}$  is in meters per second, slope gradient  $s$  is in meters/meter, coefficients  $a_0$  and  $a_1$  are given in Figure 8, and  $\overline{\ln(V_{S30})}$  is the model prediction for a given set of coefficients and gradient. Although the Pleistocene and Holocene fits lie above and below the Quaternary fit, respectively, only the Pleistocene fit lies outside of the 95% confidence intervals for the Quaternary. Additional analyses have been undertaken for 30 arcsec gradient with similar results but slightly flatter slopes ( $a_1$ ). We adopt the 3 arcsec gradient due to its slightly stronger correlation with  $V_{S30}$  in Quaternary sediments (i.e., higher  $a_1$  terms) and slightly lower standard deviations for the Holocene and Pleistocene age groups ( $\sigma_{\ln V} = 0.36$  and 0.41 for 30 arcsec, as compared to 0.35 and 0.39 for 3 arcsec for the Holocene and Pleistocene, respectively).

A similar set of plots and fits are shown for the Tertiary and Mesozoic age groups in Figure 9. Because the Tertiary results are very similar to those for the Pleistocene, these two age groups were combined for regression, with the resulting fit and confidence intervals shown in the figure. The Mesozoic velocities do not have a significant trend with gradient, hence the use of the category mean from Figure 7 is recommended over the power law relationship. A similar lack of trend in velocity with gradient for Mesozoic sites was found by Wald *et al.* (2011).

*Effects of Material Gradation and Depositional Environment.* To investigate possible effects of material gradation,

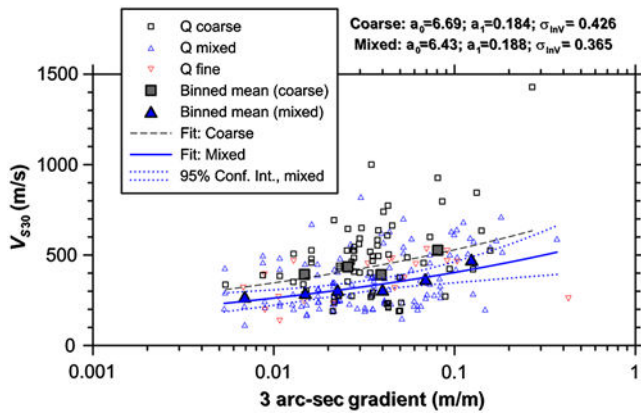


**Figure 10.**  $V_{S30}$  compared with gradient for Quaternary sediments, sorted by material gradation. Binned means and fit curves per power law relationship (equation 4) are shown for the well-populated coarse and mixed groups. The coarse fit is above the 95% confidence intervals for the mixed group, so the two categories are judged to be distinct. The color version of this figure is available only in the electronic edition.

we plot the Quaternary data in Figure 10 (as in Fig. 8) with the data points segregated according to coarse, fine, and mixed gradations. The data reflect the expected pattern of coarse sites at steeper gradients and fine/mixed sites at flatter gradients. Also shown are power law fits (equation 4) for the coarse and mixed gradation groups. The fine gradation group is poorly populated but is generally similar to the mixed group. The coarse fit falls well above the confidence intervals for the mixed fit, indicating that the differences between these groups are statistically significant. The coarse group also has higher dispersion than most geologic categories considered previously. Although not shown in Figure 10 directly, the mixed fit is quite close (yet slightly lower) than the Quaternary fit in Figure 8. The corresponding regression coefficients for the two well-populated classes are given in Figure 10. Until more information becomes available, the fine group can be approximated using coefficients for the mixed group. Overall, these data indicate that material gradation is a viable indicator for  $V_{S30}$  estimation in Quaternary sediments. For Tertiary sites, the material gradations are almost entirely mixed and fine (with similar means); the coarse group contains only seven sites in this case. Accordingly, we have not developed gradation-based fits for Tertiary sites.

The gradation-based Quaternary coefficients given in Figure 10 do not account for the previously observed trend of Pleistocene sites having relatively fast velocities as compared to other Quaternary sites (Fig. 8). To investigate Pleistocene misfit, we compute velocity residuals ( $R_V$ ) as

$$R_V = \ln(V_{S30}) - \overline{\ln(V_{S30})}. \quad (5)$$

Figure 11 indicates these residuals for Pleistocene sites, which have a flat trend with respect to gradient and a bias (i.e., mean of residuals,  $\bar{R}_V$ ) of 0.145, indicating model underprediction. As also indicated in the figure, residuals for

all other age groups are practically zero. The bias for the Pleistocene can be removed by adding 0.145 to  $a_0$  for these sites when using the material gradation equations.

We were unable to consider depositional environment as a means by which to parse the Quaternary data because the vast majority of sites (87%) are fluvial, with the remainder mixed among various categories (mostly lacustrine). Because meaningful statistics could not be compiled for these other categories, we have no basis for judging distinction from fluvial. For Tertiary sites, the situation is marginally better, although in this case it is the fluvial category that is sparsely populated with nine sites. We present histograms for fluvial and (the relatively well-populated) lacustrine groups in Figure 12. As expected, lacustrine sites are softer on average than fluvial, but more data will be needed before proxies that consider depositional environment can be provided.

*Recommended Geology-Based Approach for  $V_{S30}$  Estimation.* When  $V_{S30}$  is to be estimated using a geology-based proxy within the study region (Greece), we recommend the following:

1. Quaternary sediments: Use equation (4) with the applicable gradation group and its associated coefficients in Figure 10.
  - Exception: If the Quaternary age is Pleistocene, add 0.145 to the  $a_0$  values in Figure 10.
  - If material gradation is unknown and the geologic age is Holocene or Quaternary (subgroup not specified), use equation (4) with the “all Q” coefficients in Figure 8.
  - If material gradation is unknown and geologic age is Pleistocene, use equation (4) with the “P&T” coefficients in Figure 9.
2. Tertiary rock sites: Use equation (4) with the “P&T” coefficients in Figure 9.
3. Mesozoic sites: Use the category mean of 589 m/s (equivalent to  $a_0 = 6.378$  and  $a_1 = 0$ ).

## Implementation

### Proxies and Weighting

Best practices in site characterization are to develop full  $V_S$  profiles (extending to rock) derived from geophysical data. When it is necessary to estimate  $V_{S30}$  for sites lacking such data, given currently available proxy relationships (including those in this paper), there are three options for sites in Greece: (1) the gradient-based approach of Wald and Allen (2007), (2) the terrain-based approach of Yong *et al.* (2012) with the updated category means shown in Figure 5, and (3) the geology and gradient proxy presented in the previous section.

We recommend use of the latter two approaches, not the gradient-only approach of Wald and Allen (2007). That approach is marginally less desirable due to misfit in some gradient groups (Fig. 6) and modest correlation between the

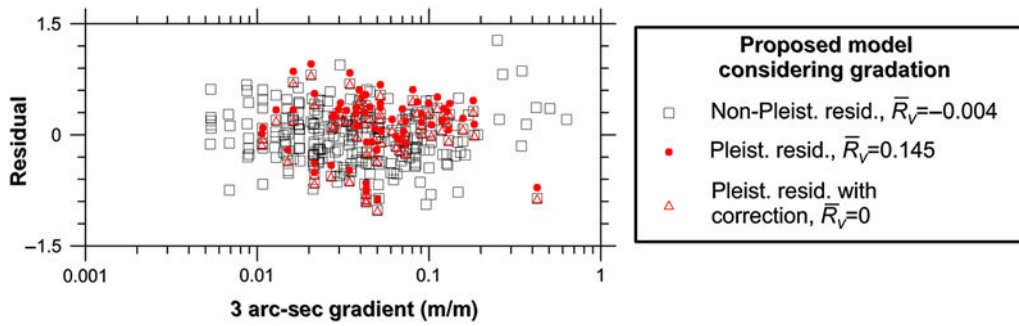


**Figure 11.** Residuals compared with the gradient for non-Pleistocene and Pleistocene sites. Data residuals are computed relative to proposed power law relationship (equation 4). Gradation-based coefficients are applied for the Quaternary. For the Tertiary and Mesozoic, we apply T coefficients from Figure 9 and the binned mean from Figure 7, respectively. The color version of this figure is available only in the electronic edition.

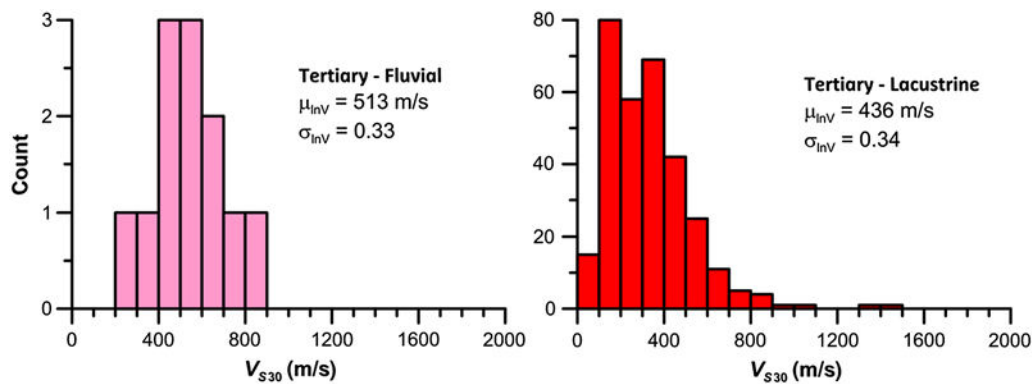


**Figure 12.**  $V_{S30}$  values from Tertiary sites, sorted by depositional environment. We consider the data to be too sparse to consider depositional environment for  $V_{S30}$  estimation. The color version of this figure is available only in the electronic edition.

30 arcsec slope gradients and the 3 arcsec gradients considered in the proposed geology-based proxy (the approximate range of correlation coefficients is 0.3–0.6 depending on geologic category). It should be emphasized that because the Wald and Allen (2007) approach is based on a globally available proxy, it will be the only practical approach for many regions around the world. Our recommendation of alternates in this case is predicated on the availability of a suitable local proxy relationship.

Because we are recommending two proxy methods, there will be two estimates of  $V_{S30}$  for any given site lacking measurements. Protocols developed in the NGA-West 2 project (Seyhan *et al.*, 2014) are to compute a weighted average of available proxy-based  $V_{S30}$  values, with the weights inversely related to the residual sum of squares (i.e.,  $\bar{R}_V^2 + \sigma_{inV}^2$ ). In our case, the mean biases ( $\bar{R}_V$ ) are practically zero, because the proxies are applied in the region that produced the data used in their development. Thus, the weights are dependent only on the variance of residuals ( $\sigma_{inV}^2$ ). The overall standard deviations for the two approaches are 0.396 and 0.394, respectively. Given that these are practically identical, the two proxies can be equally weighted.

#### Standard Deviation of $V_{S30}$ for Sites with Measurements

When multiple  $V_S$  profiles are developed for a given site, between-profile variations of  $V_S$  will be encountered and different  $V_{S30}$  values will be computed for each profile. The  $V_{S30}$  dispersion among profiles is denoted  $\sigma_{inV}$ , as with the proxies.

In the NGA-West 2 project,  $\sigma_{inV}$  was computed for sites in active crustal regions worldwide having multiple measurements. Separation distances were on the order of 10 to about 100 m, and only measurement methods considered reliable were used. As described by Seyhan *et al.* (2014), these calculations showed that variations among measurement types were small and the principal factor causing high variability is when the surface geology is variable across the site. Excluding such conditions, the range of  $\sigma_{inV}$  was approximately 0.02–0.12, with an average of about 0.06. A value of 0.1 was applied to sites with measurements in the NGA-West 2 site database.

There are eight clusters of sites in Greece where this analysis can be applied, with the results in Table 4. The values of  $\sigma_{inV}$  range from 0.02 to 0.16, with an average of 0.09.

Table 4

Clusters of  $V_S$  Profiles for which Group Statistics can be Computed. (Spacing between Profiles is Generally 100 m or Less.)

Site Cluster (3 or more)	$V_{S30}$ Values (m/s)	$\mu_{ln V}$	$\sigma_{ln V}$
AIGAMY: 002a, 004c, 003d, 003a	463, 545, 466, 524	498	0.083
ATHPIR047: a, b, c	514, 547, 701	582	0.164
ATHPIR: 054b, 055a, 056b, 057b	299, 267, 280, 329	293	0.090
KALKAL: 006a, 007a, 008a	402, 518, 525	478	0.150
KORKOR: 001a, 001b, 001c	356, 333, 374	354	0.058
LEFLEF: 001a, 002a, 003e	218, 273, 276	254	0.133
PATPAT: 010a, 011a, 012a, 012e	376, 381, 369, 385	378	0.018
VLVZAG: 007e, 008a, 008c, 008e	234, 217, 234, 210	224	0.044

These results support the value of 0.1 applied in NGA-West 2.

Protocols for Assigning  $V_{S30}$  and Its Uncertainty

The results of this research will be applied subsequently for establishing a site database for recording stations in Greece. On the basis of the findings presented here, a value of  $V_{S30}$  and its uncertainty can be assigned to any site with a known location, as given in Table 5.

Discussion and Conclusions

The time-averaged shear-wave velocity in the upper 30 m of a site ( $V_{S30}$ ) is commonly used as the principal site parameter for ground-motion prediction. Parameter  $V_{S30}$  and other metrics of site condition used in GMPEs (principally depth to a  $V_S$  horizon) are best developed from site-specific measurements. However, it is common that such data are unavailable, which necessitates  $V_{S30}$  estimation from proxies. Because of regional variations in geologic conditions, proxy-based estimation of  $V_{S30}$  is best undertaken at a local level, as seemingly similar conditions in different regions can have different velocity structures. This has been shown in past work to be particularly true for rock-site conditions (Scasserra *et al.*, 2009).

In this paper, we describe the results of a large project having the goal of enabling reliable, proxy-based estimates that are customized for a local region (in this case, Greece).

The process begins with the exacting task of assembling a database of  $V_S$  profiles, the PDB. Our PDB was compiled from published sources and a variety of research and engineering reports. It contains 314 sites, 238 of which have profile depths of 30 m or more and 59 of which are near (within 100 m) strong-motion stations. In addition to basic site information (name, location), the PDB includes information on geophysical test type, profile depth, time-averaged shear-wave velocity to the profile depth ( $V_{SZ}$ ), and  $V_{S30}$ . We utilize the data for sites with profile depths  $z_p \geq 30$  m to test  $V_{SZ}$ -to- $V_{S30}$  extrapolation methods from the literature that have been developed principally from data from California and Japan. We find these models overpredict  $V_{S30}$  for Hellenic sites, suggesting flatter gradients in Greece. We present depth-dependent linear models for performing this extrapolation. We also use the subset of the data having profile depths significantly more than 30 m to illustrate a phenomenon widely observed elsewhere—the strong correlation of  $V_{S30}$  to time-averaged velocities for greater depths. We demonstrate this feature using a profile depth of 60 m.

A major aspect of our project was to compile proxies for all PDB sites, including ground slope gradient at 30 and 3 arcsec resolution, terrain type as given by Iwahashi and Pike (2007), and surface geology. Surface geology was a particular challenge, due principally to lack of consistent naming conventions for geologic units. We overcame this problem by consulting with a network of local expert geologists to develop uniform criteria for characterization of local geology for use in  $V_S$ -related applications. The results, given in Table 2, provide five age categories, three material gradation categories, and 22 depositional environment categories. The most well-populated conditions are Quaternary sediments of coarse or mixed gradation, derived from fluvial or lacustrine depositional environments. There are also a significant number of rock sites, mostly in the Tertiary age group (Neocene).

We plot the data against the Wald and Allen (2007) gradient-based model, and find the model to overpredict the  $V_{S30}$  data for 30 arcsec gradients  $> \sim 0.05$  m/m. Bias is also found for four of the eight well-populated geomorphic categories, and new values are provided when previous values from Yong *et al.* (2012) are rejected by the data. These differences confirm the presence of variable geophysical conditions, even for apparently similar geology, in the local

Table 5  
Recommended Protocols for Assigning  $V_{S30}$  and Its Uncertainty to Recording Stations

Code	Data Source Type
0	Assign from measured velocity profile with $z_p \geq 30$ m in proximity of site (within approximately 100 m). $\sigma_{ln V} = 0.1$ .
1	Estimate from measured velocity profiles with depths $10 \leq z_p < 30$ m and located within approximately 100 m using $V_{SZ} - V_{S30}$ relationships described above. $\sigma_{ln V} = \sqrt{0.1^2 + \sigma_e^2(z_p)}$ , in which the depth-dependent $\sigma_e$ is from Table 1.
2	Estimate from velocity profile at a different site but in the vicinity of instrument (generally within 1 km) on the same surface geology. $\sigma_{ln V} = 0.2$ if $z_p \geq 30$ m. $\sigma_{ln V} = \sqrt{0.2^2 + \sigma_e^2(z_p)}$ if $z_p < 30$ m.
3	Inferred from average of terrain- and geology-related proxies as given above ( $\sigma_{ln V} = 0.4$ ).

The lowest code number that can be applied given the available site data should be used.

application region of Greece as compared to California and Japan (where most of the prior data was derived).

We develop a geology-based  $V_{S30}$  estimation procedure by plotting the data within geologic classes against gradient. We find that gradients measured at 3 arcsec resolution produce stronger trends (i.e., steeper slopes in  $V_{S30}$ -gradient space), and reduced dispersion, than results for 30 arcsec. We find an effect of gradient for Quaternary and Tertiary materials, but no gradient effect for those from the Mesozoic. Among Quaternary sediments, Holocene, mapped Quaternary (age unspecified), and mixed/fine gradation materials exhibit reasonably consistent  $V_{S30}$ -gradient trends, whereas Pleistocene and coarse-gradient sediments exhibit faster velocities. We develop a simple procedure for  $V_{S30}$  estimation that considers these factors. For application, we recommend giving equal weight to estimates from the modified terrain-based method and the proposed geology-based method.

One of the principal applications of a PDB and proxies for  $V_{S30}$  estimation is to establish site parameters for use in the development of GMPEs. Such applications require site parameters at each recording station. We provide protocols that emphasize the use of data when they are available and proxies otherwise. We also provide recommendations on the uncertainty of  $V_{S30}$ , which is established from residuals analysis for the proxies, and from analysis of clustered  $V_S$  profiles for  $V_{S30}$  established from data. The results are used for ongoing ground-motion research conducted for Greece.

Limitations of our study are that certain geologic conditions are poorly represented (especially hard rock), and site parameters considered in some GMPEs are not addressed directly (site period and the depth to shear-wave horizon).

## Data and Resources

The velocity profile data utilized in this study are derived from a variety of sources, including the open literature, research reports, and reports from private consulting engineers and government offices. © Sources for individual profiles are given in the electronic supplement materials. The information directly used in the analyses presented in this paper is presented in its entirety in the electronic supplement.

The following digital elevation models (DEMs) were used to obtain gradients considered in this study: a near-global, 30-arcsec-resolution, DEM comprising a combination of data from the Shuttle Radar Topography Mission (SRTM), flown in February 2000, and the U.S. Geological Survey (USGS) GTOPO30 data set (<https://lta.cr.usgs.gov>; last accessed May 2014); 9 arcsec resolution model obtained from ACE2 (<http://tethys.eaprs.cse.dmu.ac.uk/ACE2/>; last accessed May 2014), which is also SRTM based; a 3 arcsec DEM from USGS SRTM Digital Terrain Elevation Data (DTED) Level 1 (<https://lta.cr.usgs.gov>; last accessed May 2014); and a 1 arcsec DEM, from the National Aeronautics and Space Administration website, *The Advanced Spaceborne Thermal Emission and Reflection Radiometer (ASTER) Global Digital Elevation Model (GDEM)* ([\[asterweb.jpl.nasa.gov/\]\(http://asterweb.jpl.nasa.gov/\); last accessed May 2014\). SRTM data at 1 arcsec resolution are not available for Greece from the USGS. Gradients were computed from elevation data using the \*grdgradient\* command in Generic Mapping Tools software \(<http://gmt.soest.hawaii.edu/>, last accessed May 2014\).](http://</a></p>
</div>
<div data-bbox=)

Elevation data used for the validation of DEM-based gradients were obtained from the Hellenic Military Geographical Service, National Trigonometric Network website ([http://web.gys.gr/portal/page?\\_pageid=33,36834&\\_dad=portal&\\_schema=PORTAL](http://web.gys.gr/portal/page?_pageid=33,36834&_dad=portal&_schema=PORTAL); last accessed May 2014).

The geology discussed in our work was based on various maps from the Institute of Geological and Mineral Exploration (IGME), available as *Geologic Sheets of Greece in 1:50,000 scale*, [www.igme.gr](http://www.igme.gr) (last accessed May 2014).

## Acknowledgments

This research was partially co-funded by the following research projects: (1) European Union (European Social Fund [ESF]) and Hellenic national funds through the Operational Program “Education and Lifelong Learning” of the National Strategic Reference Framework (NSRF)—Research Funding Program “THALES” (MIS 377335); (2) European Neighborhood and Partnership Instrument (ENPI) and Hellenic national funds in the framework of the cross-border cooperation program, Black Sea Basin Joint Operational Project 2007–2013 (MIS-ETC 2614); and (3) “ARCHIMIDIS III: Research Teams Reinforcement in ASPETE” (MIS 383576) of the Operational Program “Education and Lifelong Learning,” co-funded by the European Union and national funds.

We extend sincere thanks to the panel of geologists who assisted with the assignment of geologic categories for profile database (PDB) sites, including V. Marinos, P. Marinos, K. Papatheodorou, D. Rozos, N. Nikolaou, and K. Dimaras. We also thank R. E. Kayen, who assisted with  $V_S$  profiling for some sites in the PDB, and Dimitri Atmatzidis who assisted in the procurement of essential equipment for  $V_S$  profiling. Students T. Bika, F. Kapeti, and A. Kokkinou of the Institute of Engineering Seismology & Earthquake Engineering (Greece), as well as E. Psaroudakis, K. Iordanis, El. Petala, Th. Lazaridis, Ch. Charharidi, and K. Mimidis of the Democritus University of Thrace, who assisted in the compilation of the PDB. Finally we thank David Wald of the U.S. Geological Survey and one anonymous reviewer for their insightful comments.

## References

- Allen, T. I., and D. J. Wald (2009). On the use of high-resolution topographic data as a proxy for seismic site conditions ( $V_{S30}$ ), *Bull. Seismol. Soc. Am.* **99**, 935–943.
- Boore, D. M. (2004). Estimating  $V_{S30}$  (or NEHRP site classes) from shallow velocity models (depths < 30 m), *Bull. Seismol. Soc. Am.* **94**, 591–597.
- Boore, D. M., E. M. Thompson, and H. Cadet (2011). Regional correlations of  $V_{S30}$  and velocities averaged over depths less than and greater than 30 m, *Bull. Seismol. Soc. Am.* **101**, 3046–3059.
- Borcherdt, R. D. (1970). Effects of local geology on ground motion near San Francisco Bay, *Bull. Seismol. Soc. Am.* **60**, 29–61.
- Borcherdt, R. D. (1994). Estimates of site-dependent response spectra for design (methodology and justification), *Earthq. Spectra* **10**, 617–653.
- Bozorgnia, Y., N. A. Abrahamson, L. Al Atik, T. D. Ancheta, G. M. Atkinson, J. W. Baker, A. Baltay, D. M. Boore, K. W. Campbell, B. S.-J. Chiou, *et al.* (2014). NGA-West2 research project, *Earthq. Spectra* **30**, 973–987.
- Castellaro, S., F. Mulargia, and P. L. Rossi (2008).  $V_{S30}$ : Proxy for site amplification? *Seismol. Res. Lett.* **79**, 540–543.
- Chiou, B. S.-J., R. Darragh, D. Dreger, and W. J. Silva (2008). NGA project strong-motion database, *Earthq. Spectra* **24**, 23–44.



- Fumal, T. E. (1978). Correlations between seismic wave velocities and physical properties of near-surface geologic materials in the southern San Francisco Bay region, California, *U.S. Geol. Surv. Open-File Rept. 78-1067*, 114 pp.
- Fumal, T. E., and J. C. Tinsley (1985). Mapping shear wave velocities of near surface geologic materials, in *Evaluating Earthquake Hazards in the Los Angeles Region—An Earth-Science Perspective*, J. E. Ziony (Editor), *U.S. Geol. Surv. Profess. Pap. 1360*, 101–126.
- Higgins, M. D., and R. Higgins (1996). *A Geological Companion to Greece and the Aegean*, Duckworth Publishers, Ithaca, New York.
- Iwahashi, J., and R. J. Pike (2007). Automated classifications of topography from DEMs by an unsupervised nested-means algorithm and a three-part geometric signature, *Geomorphology* **86**, nos. 3/4, 409–440.
- Kottke, A. R., Y. M. A. Hashash, J. P. Stewart, C. J. Moss, S. Nikolaou, E. M. Rathje, W. J. Silva, and K. W. Campbell (2012). Development of geologic site classes for seismic site amplification for central and eastern North America, *Proc. 15th World Conf. on Earthquake Eng.*, Lisbon, Portugal, 24–28 September 2012, Paper Number 4557.
- Lee, C.-T., C.-T. Cheng, C.-W. Liao, and Y.-B. Tsai (2001). Site classification of Taiwan free-field strong-motion stations, *Bull. Seismol. Soc. Am.* **91**, 1283–1297.
- Lemoine, A., J. Douglas, and F. Cotton (2012). Testing the applicability of correlation between topographic slope and  $V_{S30}$  for Europe, *Bull. Seismol. Soc. Am.* **102**, 2585–2599.
- Matsuoka, M., K. Wakamatsu, F. Fujimoto, and S. Midorikawa (2006). Average shear-wave velocity mapping using Japan engineering geomorphologic classification map, *J. Struct. Mech. Earthq. Eng.* **23**, 57s–68s.
- Mountrakis, D. M. (1985). *The Geology of Greece*, University Studio Press, Thessaloniki, Greece.
- Nikolakopoulos, K., and P. Tsombos (2010). Updating the 1:50,000 geological maps of IGME with remote sensing data, GPS measurements and GIS techniques: The case of Antiparos Island, in *Remote Sensing for Science, Education, and Natural and Cultural Heritage (EARSEL)*, R. Reuter (Editor), European Association of Remote Sensing Laboratories, Paris, France, 281–287.
- Park, S., and S. Elrick (1998). Prediction of shear wave velocities in southern California using surface geology, *Bull. Seismol. Soc. Am.* **88**, 677–685.
- Scasserra, G., J. P. Stewart, R. E. Kayen, and G. Lanzo (2009). Database for earthquake strong motion studies in Italy, *J. Earthq. Eng.* **13**, 852–881.
- Seyhan, E., J. P. Stewart, T. D. Ancheta, R. B. Darragh, and R. W. Graves (2014). NGA-West2 site database, *Earthq. Spectra* **30**, 1007–1024.
- Stewart, J. P., A. H. Liu, and Y. Choi (2003). Amplification factors for spectral acceleration in tectonically active regions, *Bull. Seismol. Soc. Am.* **93**, 332–352.
- Wald, D. J., and T. I. Allen (2007). Topographic slope as a proxy for seismic site conditions and amplification, *Bull. Seismol. Soc. Am.* **97**, 1379–1395.
- Wald, D. J., L. McWhirter, E. Thompson, and A. Hering (2011). A new strategy for developing  $V_{S30}$  maps, *Proc. 4th Int. Effects of Surface Geology on Seismic Motion Symp.*, Santa Barbara, California, 23–26 August 2011, 12 pp.
- Wills, C. J., and K. B. Clahan (2006). Developing a map of geologically defined site-condition categories for California, *Bull. Seismol. Soc. Am.* **96**, 1483–1501.
- Wills, C. J., and C. Gutierrez (2008). Investigation of geographic rules for improving site-conditions mapping, *Calif. Geo. Sur. Final Tech. Rept. 20* pp. (Award Number 07HQGR0061).
- Yong, A., S. E. Hough, J. Iwahashi, and A. Braverman (2012). Terrain-based site conditions map of California with implications for the contiguous United States, *Bull. Seismol. Soc. Am.* **102**, 114–128.
- Zargli, E., S. Liodakis, P. Kyriakidis, and A. Savvaidis (2013). Classification of topography using DEM data and its correlation with the geology of Greece, *1st Int. Conf. on Remote Sensing and Geoinformation of the Environment (RSCy2013)*, D. G. Hadjimitsis, K. Themistocleous, S. Michaelides, and G. Papadavid (Editors), Proc. of SPIE, Vol. 8795, 87950S.

Department of Civil and Environmental Engineering  
University of California  
5731 Boelter Hall  
Los Angeles, California 90095-1593  
(J.P.S.)

Democritus University of Thrace (D.U.Th.)  
Department of Civil Engineering  
12, Vassilissis Sophias Street  
GR-67100 Xanthi, Greece  
(N.K.)

Institute of Engineering Seismology and Earthquake Engineering (ITSAK-EPPO)  
P.O. Box 53 Finikas  
GR-55102 Thessaloniki, Greece  
(A.S., N.T., E.Z., B.M.)

Department of Civil Engineering  
University of Patras  
GR-26500 Patras (Rion), Greece  
(G.A.)

School of Pedagogical and Technological Education (ASPETE)  
Department of Civil Engineering  
GR 141 21, N. Heraklion, Greece  
(P.P.)

University of Bristol  
Department of Civil Engineering  
University Walk Bristol  
Bristol BS8 1TR, United Kingdom  
(G.M.)

Manuscript received 24 December 2013;  
Published Online 21 October 2014